Study on the mechanism of seismic damage of historical burial mounds

Mai Sawada[1], T. Enkhtuvshin[1], and M. Mimura[1]

[1] Graduate School of Engineering, Kyoto University, Kyoto daigaku-Katsura, Nishikyo-ku, Kyoto 615-8540, Japan

ABSTRACT

Burial mounds constructed more than 1300 years ago in Japan have been seriously damaged by earthquakes. The development of prevention measures for seismic damage of burial mounds are required to conserve them for the next generation. In the present study, dynamic centrifuge model tests were conducted to study the mechanism of seismic damage of burial mounds. In a burial mound model after shaking, the displacement of the sidewall of the burial chamber and the collapse of its backfill were observed. As well as the remarkable damage of the chamber, cracks were found in the surface of the mound and the upper corners of the chamber. The model tests were simulated by numerical analyses to investigate the mechanism of the formation of the cracks. The numerically predicted tensile crack areas and crack directions exactly agreed with the experimentally observed ones.

Keywords: conservation of geoheritages, centrifuge model test, dynamic response analysis

1 INTRODUCTION

From the middle of the 3rd century to the end of the 7th century in Japan, many burial mounds were constructed for the imperial family and district rulers. They have been conserved as geoheritages, but they are damaged by natural forces and human activities. Earthquakes particularly cause serious damage; cracks and failures in mounds, rockfall in burial chambers, water infiltration through cracks, etc. The burial mound shown in Fig. 1 was damaged by the 2016 Kumamoto Earthquake (M 7.3).

To protect burial mounds from earthquakes, studies on the mechanism of seismic damage and the development of prevention measures are strongly required. In the present study, the mechanism of seismic damage of burial mounds is discussed based on dynamic centrifuge model tests and numerical analyses.

Fig. 1. A burial mound damaged by the 2016 Kumamoto Earthquake (Agency for Cultural Affairs and Education Bureau of Kumamoto pref. 2017).

2 DYNAMIC CENTRIFUGE MODEL TEST

2.1 Burial mound model

A series of centrifuge model tests under 50 g was conducted on a 1/50 scale model of a cross-section of a burial mound as shown in Fig. 2. The scaling factors are listed in Table 1. The properties of the model summarized in Table 2 were determined by referring to the geotechnical investigations in the Takamatsuzuka Tumulus in Nara prefecture. (Mimura and Ishizaki 2006). The model was prepared by compacting the decomposed granite soil with rich fine fraction (F_c=42%) sampled in the similar tumulus mound near the Takamatsuzuka Tumulus. The burial chamber in the mound model was simulated with four resin boards of which density is same as the tuff used for actual burial chambers. The boards were not adhered each other.

Acceleration was measured with accelerometers at the shaking table and three points shown in Fig. 2. The settlement of the crest and the horizontal displacement

Table 1. Scaling factors (=Prototype / Model).

	Dimension	Scaling factor

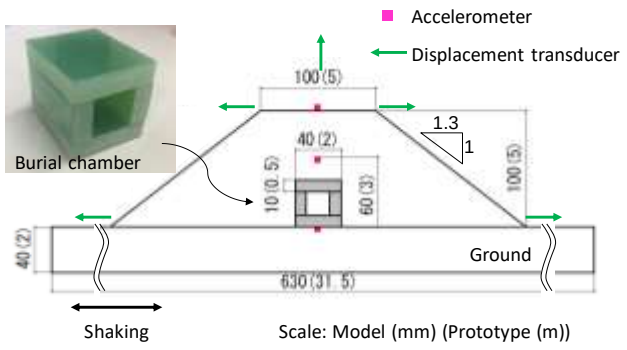

Fig. 2. The burial mound model for centrifuge model tests.

Length	L	N
Mass	M	N^3
Time	T	N
Acceleration	LT^{-2}	N^{-1}
Stress	$ML^{-1}T^{-2}$	1
Strain	—	1

Table 2. Properties of the burial mound model.

	Mound	Ground
Wet density (g/cm^3)	1.58	1.91
Water content (%)	15	—
Degree of saturation (%)	43	—
Shear modulus (MN/m^2)	27	119
Shear velocity (m/s)	130	250

of the toe and top of the slope were measured with laser-displacement transduces.

2.2 Test cases

The tests were conducted in the geotechinical centrifuge of the Disaster Prevention Research Institute of Kyoto University, Japan, which is equipped with a shaking table. Sinusoidal waves with different amplitude were employed in increasing order. The frequency of the waves was fixed at 2Hz in prototype scale. In what follows, units are in prototype.

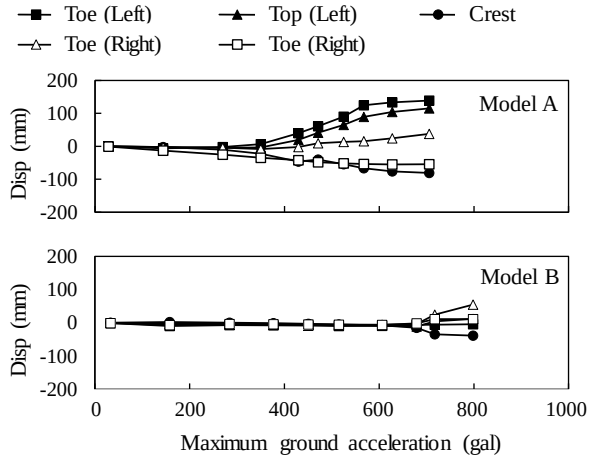

Fig. 4. Residual displacement of the mound accumulated in 10 successive shaking.

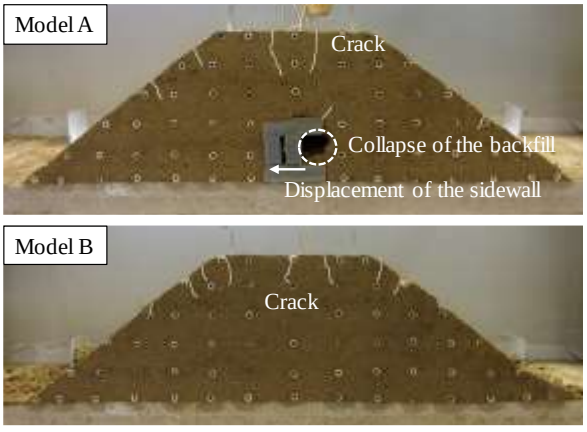

Fig. 3. Damaged burial mound models after shaking.

In addition to the model shown in Fig. 2, a model without a burial chamber was also employed to discuss the contribution of a chamber to the dynamic behavior of the mound. The properties of the model without a burial chamber are same as those in Table 2. Note that the model in Fig. 2 and the model without a burial chamber are hereinafter referred to as Model A and Model B, respectively.

2.3 Test results

Fig. 3 shows typically damaged models after shaking. The sidewall of the burial chamber of Model A slid inside of the chamber and the backfill collapsed. In addition to the remarkable damage of the chamber, cracks are found in the surface of the mound and the upper corner of the burial chamber. The surface cracks are also found in Model B.

Residual displacement of the mound accumulated in 10 successive shaking is shown in Fig. 4. Here, a positive value represents a displacement in the arrow directions shown in Fig. 2. The curves describe that the crest settles down and the toe and top of the slope extend laterally. The displacement of Model A and Model B indicates a similar tendency, but the mound of Model A with the chamber is easy to deform.

Fig. 5 shows the response acceleration of Model A observed in the fourth shaking of the 10 successive shaking. The amplitude factor of each measurement points are shown in Table 3. Here, amplitude factor is defined as the ratio of Fourier amplitude at 2Hz (hereinafter called *Amp* $_{2Hz}$) of the response acceleration at a measurement point to *Amp* $_{2Hz}$ of the input acceleration observed at the shaking table. The amplitude factor of the Model A is remarkably larger than Model B. The difference in amplitude factors agrees with the fact that the existence of a burial chamber contributes to larger deformation.

Table 3. Amplitude factor.

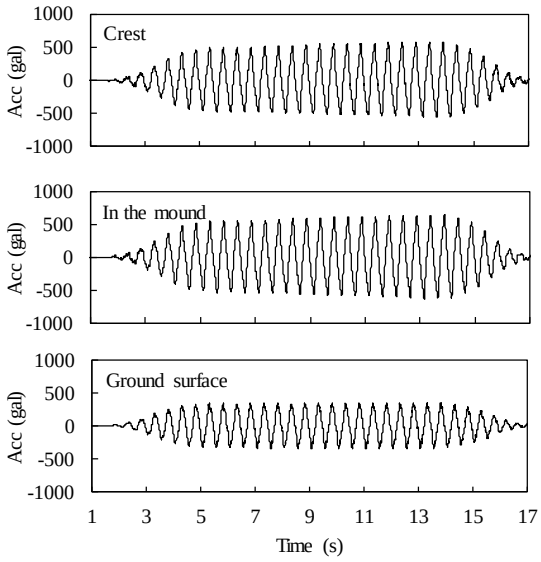

Fig. 5. Measured time histories of acceleration (Model A).

	Ground surface	In the mound	Crest
Model A	1.2	2.4	2.5
Model B	1.2	1.7	1.6

3 NUMERICAL ANALYSIS OF THE CENTRIFUGE MODEL TEST

3.1 Numerical model

To investigate the mechanism of the damage of the burial mound observed by the centrifuge model tests, the model tests on Model A is calculated by FEM analysis (LIQCA2D17, The LIQCA Research and Development Group 2017).

The modified Ramberg-Osgood model (Japanese Geotechnical Society 1999), a total stress model considering the non-linearity of hysteretic stress-strain curves in cyclic loading, is applied to the mound because the degree of saturation is relatively low and the cracks observed by the model test is probably induced by the inertia force rather than excess pore water pressure. The skeleton curve and hysteresis curve are expressed in Eq. (1) and Eq. (2), respectively.

$$\gamma = \frac{\tau}{G_{\max}}\left(1+\alpha\left|\frac{\tau}{\tau_f}\right|^{r-1}\right) \quad (1)$$

$$\frac{d\tau}{d\gamma} = \frac{G_{\max}}{1+\alpha r\left|\frac{\tau-\tau_r}{2\tau_f}\right|^{r-1}} \quad (2)$$

Here, τ: shear stress, τ_r: shear stress at loading direction reverses, and G_{max}: maximum shear modulus.
The model parameters, α and r, are determined by referring to the deformation properties obtained by cyclic triaxial tests. Shear modulus G and damping constant h are expressed as follows.

$$h = \frac{2(r-1)}{\pi(r+1)}\left(1-\frac{G}{G_{\max}}\right) \quad (3)$$

$$\frac{G}{G_{\max}} = \frac{1}{1+\alpha\left|\frac{\tau}{\tau_f}\right|^{r-1}} \quad (4)$$

Joint elements are introduced to the contact between the chamber boards and the contact between the boards and backfill to express a slip and split at the contact. Here, the boards are assumed to be rigid.

The test cases with three different input waves (hereinafter referred to as Case 1, Case 2 and Case 3 in increasing order of amplitude) are numerically analyzed. The acceleration observed at the ground surface in the model tests is given at the bottom of the numerical mound model. Note, in the model test, smaller shaking had been given before these three cases, but significant plastic deformation was not observed in the previous shaking.

3.2 Comparison of the experimentally and numerically obtained response accelerations

The response accelerations obtained by the model tests and the numerical analyses are compared in Fig. 6. The numerically obtained accelerations quantitatively agree with experimentally obtained ones although the numerical analysis does not reproduce the high-frequency waves in Case 3 induced by significant damage of the mound.

4 THE MECHANISM OF THE SEISMIC DAMAGE OF BURIAL MOUNDS

4.1 Distribution of maximum shear stress

To investigate the mechanism of the formation of the cracks observed by the model tests, stress distribution in the mound is analyzed. Fig. 9 shows the distribution of the maximum shear stress τ_{max} when τ_{max} reaches a maximum in cyclostationary state. Larger τ_{max} is observed in the backfill split off from the sidewall of the chamber and τ_{max} of some elements exceeds the shear strength. However, in the surface of the mound where many cracks are found in the model test, τ_{max} is relatively small. This suggests that the cracks are induced not only by shear stress.

4.2 Distribution of minimum principal stress

Tensile stress as well as shear stress is a factor that induces the cracks. Fig. 7 shows the distribution of the minimum principal stress σ_3 when σ_3 reaches a minimum in cyclostationary state. Here, positive and negative values represent compression and tensile stress, respectively. Tensile stress is found at the surface of the

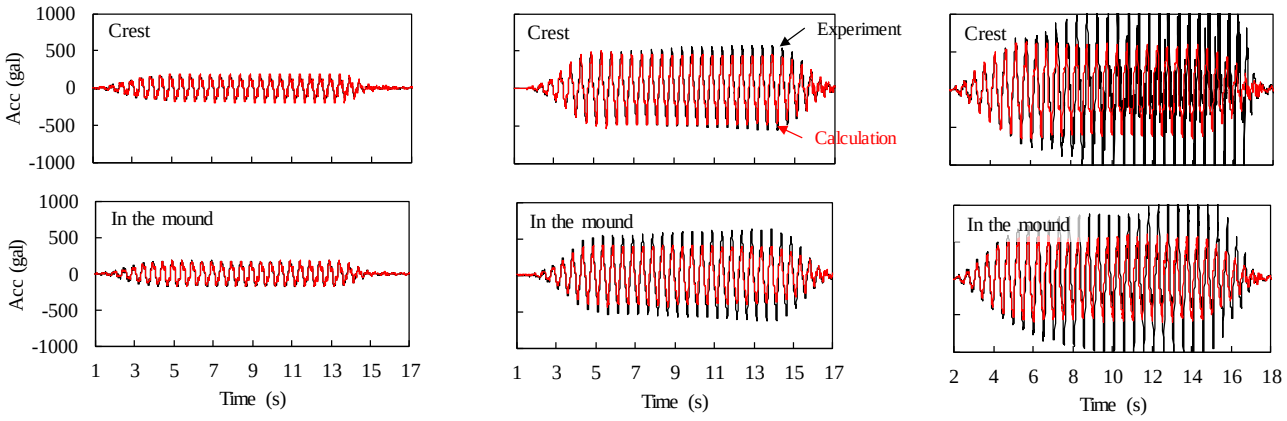

Fig. 6. Comparison of experimentally and numerically obtained response accelerations (left: Case 1, middle: Case 2, right: Case 3).

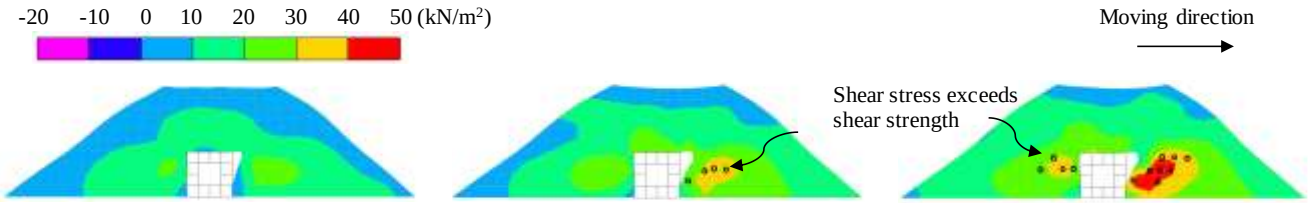

Fig. 9. The distribution of maximum shear stress (left: Case 1, middle: Case 2, right: Case 3).

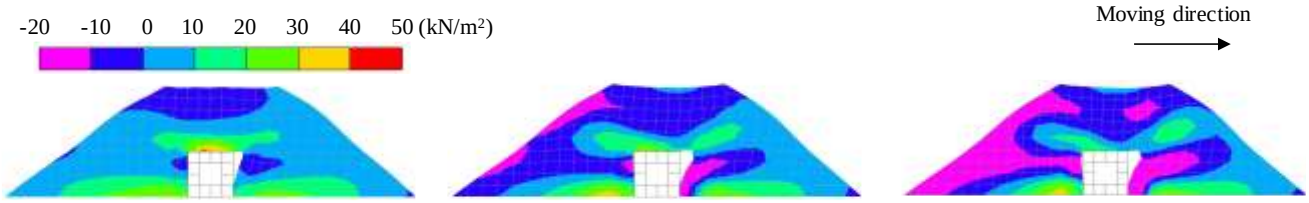

Fig. 7. The distribution of minimum principal stress (left: Case 1, middle: Case 2, right: Case 3).

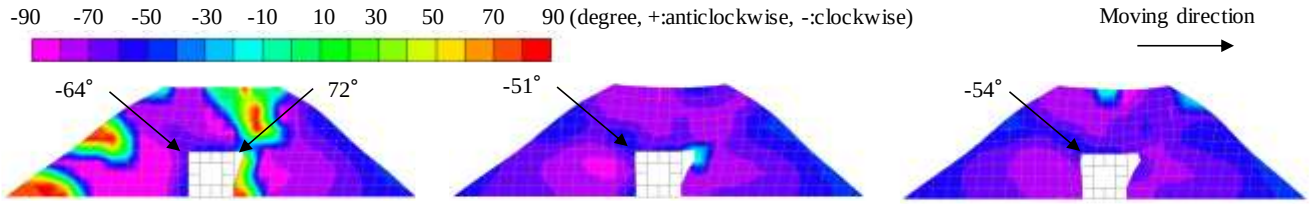

Fig. 8 The distribution of the direction of minimum principal stress plane (left: Case 1, middle: Case 2, right: Case 3).

crest and slope, and the backfill of the chamber. These tensile stress areas exactly agree with the crack areas.

Fig. 8 shows the distribution of the direction of minimum principal stress plane. In the tensile stress areas, the directions of σ_3 plane corresponds to the crack directions. For example, the tensile stress plane of the crest rotates clockwise by 70 to 90 degrees from a horizontal plane. This indicates that cracks are formed in the crest approximately in a vertical direction. Compared to the cracks shown in Fig. 3, the numerically predicted crack directions almost agree with the actual ones. This ensures that the cracks are mainly induced by tensile stress rather than shear stress.

5 CONCLUSIONS

The mechanism of seismic damages of burial mounds was investigated by dynamic centrifuge model tests. In a burial mound model after shaking, the displacement of the sidewall of the burial chamber and the collapse of the backfill were observed. As well as the significant damage of the chamber, cracks were found in the surface of the mound and the upper corners of the chamber.

The model test was also conducted on a mound model without a chamber to investigate the contribution of a burial chamber to the seismic behavior of the covering mound. The comparison with the model without a burial chamber showed that the existence of a burial chamber contributes to the amplification of vibration and larger deformation of the mound.

The mechanism of the formation of the cracks observed in the model tests was investigated with numerical analyses. The distribution of the maximum shear stress and minimum principal stress showed that the cracks were mainly induced by tensile stress. The numerically predicted tensile crack areas and crack directions exactly agreed with the experimentally observed ones.

ACKNOWLEDGEMENTS

The authors would like to express their sincere gratitude to geotechnical research groups of Kyoto University for providing equipment and giving technical advices about the centrifuge model test.

REFERENCES

Agency for Cultural Affairs and Education Bureau of Kumamoto pref. (2017). Investigation of Burial Mounds Damaged by the 2016 Kumamoto Earthquake.

Mimura. M. and Ishizaki. T. (2006). Current Status of Takamatsuzuka Tumulus and its Geotechnical Properties. Japanese Geotechnical Journal, Vol. 1, No.4. 157-168.

The LIQCA Research and Development Group. (2017). User's Manual for LIQCA2D17 and LIQCA3D17.

Japanese Geotechnical Society. (1999). Geotechnical Engineering Handbook, 212-223.

.